

Using Templates to Remove Fixed Pattern Noise from IUE Spectra

Daniel E. Welty
University of Chicago
Astronomy and Astrophysics Center
5640 S. Ellis Ave.
Chicago, IL 60637

I. Introduction

It has become apparent that there is persistent, non-random noise present in IUE spectral data which can severely limit the signal-to-noise (S/N) achievable in both individual and summed spectra. York and Jura (1982), in an early exploration of this detector-induced, so-called fixed-pattern noise (FPN), noted that the S/N in summed spectra did not increase as the square root of the number of spectra used, as would be expected from random noise alone. They also found that the noise in a single spectrum determined with respect to the mean of several spectra was generally less than the noise determined with respect to a "reasonably-drawn" mean - again implying the presence of non-random noise. It has been conjectured (Grady and Imhoff 1985; comments during this workshop) that the FPN results from noise in the intensity transfer function (ITF) and/or from misregistration of images in the construction of the ITF or in the application of the ITF to data images. Whatever the source of the FPN, however, removal of the FPN is vital for improving the S/N in IUE spectra, as its amplitude is generally comparable to the random noise present in an individual image (Adelman and Leckrone 1985 and this workshop; this paper).

Several methods have been suggested for removing FPN from IUE spectra. The first is to use many spectra obtained at different times, hoping that the spectra will exhibit different shifts relative to the fixed pattern (FP) and thus that the FPN will be largely cancelled when the spectra are added (e.g. Howarth and Phillips 1986). Another approach, somewhat similar to the first, is to make exposures with the star located at various positions in the large aperture, again hoping that different shifts of the spectra relative to the FP will lead to removal of the FPN in the summed spectra (e.g. Adelman and Leckrone 1985 and this workshop). While such methods do generally yield a reduction in the noise in the resultant spectra, their effects are somewhat unpredictable. Unfortunate combinations of spectra might leave the FPN essentially un-reduced, and, in any case, any low frequency components of the FPN (due to features in the FP

extending over more than 6-8 extracted data points) would probably not be removed. A third possible method, the use of Fourier techniques to identify and remove the FPN, is attractive in principle, but might be difficult to implement reliably unless the properties of the FPN (as described, for example, by its power spectrum) were both fairly simple and very well determined.

As much of our research using IUE data has required the accurate identification and measurement of weak absorption lines, requiring S/N typically 5 to 10 times greater than that attainable from a typical single IUE exposure, we have been investigating another technique for removing FPN from IUE spectra. We construct a "template" spectrum whose features are due primarily to the FP, then apply that template to our program star spectra to directly and explicitly remove the FPN. The explicit identification of the FP allows more reliable discrimination between real and FP-induced features in the spectra and more reliable removal of the FPN. While we have not conducted an exhaustive study of the FPN, we have used this template technique with some success on a variety of high-dispersion spectra: trailed and multiply-exposed LWR spectra (Welty, York, and Hobbs 1986), and multiply- and singly-exposed SWP and LWP spectra (Frisch, York, and Fowler 1987; Frisch, York, and Welty 1988; York, Frisch, and Welty 1988; York, Polidan, and Welty 1988). In Section II we describe the construction and use of template spectra in more detail; in Section III we present some of the results of this investigation: evidence for the existence of the FP, some of its properties, and examples of the improvement in program star spectra obtained by using this technique.

II. Procedure

The first step necessary for constructing template spectra is to choose a template star. In general, the star should be bright in the region of interest, so that short exposures may be used (minimizing problems with high background count rates and cosmic ray hits), and it should not exhibit narrow stellar or interstellar lines. Though it is not yet clear how similar in type the template star should be to the program stars, nearby unreddened early-type stars with high projected rotational velocity should generally be good candidates. The template star spectra should be positioned similarly on the detector to the program star spectra (similar positioning in the large aperture; similar dispersion constants A_1 and B_1 ?) to get a good match of the FP. It is not clear how similar the exposure levels need to be, though it would seem good to be fairly well matched. Enough exposures (typically 10 to 15) are needed to

effectively eliminate random photon noise from the constructed template spectrum.

For each image, select from the standard MEHI extracted spectra all the points in the desired order between wavelength limits λ_1 and λ_2 encompassing the region of interest. In general, λ_1 and λ_2 will correspond to different "pixels" p_1 and p_2 in the extracted spectra, where by "pixel" we will always mean "extracted data point", not picture element in the two-dimensional image. We generally choose $(\lambda_2 - \lambda_1) \sim 6$ to 12 \AA , or $(p_2 - p_1) \sim 160$ to 300 points, in order to have sufficient "continuum" to reliably identify the FP. Flatten each segment to remove stellar lines, any uncorrected echelle ripple, and any other large-scale trends or features. We typically perform a fairly high-order Legendre polynomial fit, after excising any reseaux, cosmic ray hits, "hot" pixels, etc., then divide the smooth fit into the spectrum. The resulting spectra each have mean 1.0 and fluctuations due to both random noise and FPN. Choose one of the spectra as a temporary "standard", and perform a simple cross-correlation (rms deviation as a function of relative offset in pixel space) between that standard and each individual spectrum. This generally yields for each spectrum a fairly well defined minimum rms deviation at one particular relative offset; this is taken as indicating the shift necessary to align the FP in that spectrum with the FP in the standard. Finally, use the shifts to line up the FP in all the spectra and co-add in pixel space. The random noise should be reduced by the square root of the number of spectra co-added; the fluctuations in the resulting template spectrum should reflect primarily the FP.

Program star spectra are processed similarly - each is first flattened, then cross-correlated with the template spectrum to determine the relative shift needed to align the FP in the two spectra. At this point, a "template" can be constructed from the program star spectra for comparison (of rms fluctuations, features in common) with the standard template. If the program star spectra are difficult to flatten (e.g. by virtue of narrow stellar lines), the relative shifts can be determined by deleting the hard-to-flatten sections from the flattening and cross-correlation or (almost always) by examining the relative locations of reseaux and/or other patterns in common between the template and program star spectra. Divide each program star spectrum (flattened or unflattened) by the template, after shifting the template in pixel space to align the FP, then sum the program star spectra in wavelength space. If the FP contribution to the noise is essentially the same for both the template spectrum and the program star spectra, then most of the FPN should be removed by dividing by the

template; summing the divided spectra should then reduce the remaining random noise.

III. Results

A. Evidence for the presence of a fixed pattern

For this technique to successfully remove the FPN from program star spectra, it is obviously vital that the FP be very consistent in both template and program star spectra - i.e. that the pattern is essentially fixed. There are several indications from the template construction and from the cross-correlation analysis that this is largely the case.

First, there is usually a definite minimum rms deviation in the cross-correlation of pairs of spectra. Most relative offsets yield an rms deviation comparable to that of the individual spectra; one offset (generally), however, yields an rms deviation 10% to 30% smaller. This minimum is generally more obvious when one of the spectra is the template. The minimum rms offset is almost always consistent with the relative positions in pixel space of reseaux and "hot" pixels (which are not included in the cross-correlation), as well as of other noticeably consistent patterns in the spectrum. There is generally no discernable minimum if one of the spectra has already been divided by the template.

Second, the minimum rms relative offset is generally consistent from order to order for spectra from a given pair of images, and is also consistent with the shifts introduced into the wavelength scale of each image to compensate for variations in the satellite temperature and velocity. Any slight apparent deviations from consistency in these regards may be understood by noting slight differences in the registration of pixel number with respect to the wavelength scale. These consistencies would seem to imply that the minimum rms offsets detected by the cross-correlation are indeed associated with real, persistent patterns in the spectra.

The crucial point for the utility of this technique is that the above indications seem to hold not only when comparing spectra of the same star obtained at nearly the same time, but also when comparing spectra of different stars obtained at different times. Figure 1 shows two templates constructed for a portion of order 92 of the LWR camera - one constructed from 9 images of η Lup obtained in 1982, the other from 15 images of η Lup obtained in 1983. The two templates have similar rms deviations (with respect to unity) and show

many features in common (when the relative offset, seen most easily by comparing the positions of the reseau near $\lambda 2517$, is taken into account). Figures 2 and 3 show templates constructed from several different stars for portions of orders 67 and 86, respectively, of the SWP camera. Again, many common features may be noted; the better agreement for the order 67 templates may be a consequence of having optimized the exposures for that region - variations in spectral type among the stars thus lead to differences in exposure level in order 86. (We note also that we have observed noticeably consistent patterns in weakly-exposed spectra at an amplitude larger than that in the better-exposed templates. While there is still generally a discernable minimum in the cross-correlation, it is not clear that we are seeing entirely the same pattern as in the template in those cases.) The substantial agreement shown in these three comparisons implies reasonable consistency in the location of images on the detector and in the processing of the data, and suggests that the use of templates can remove much of the FPN in at least some circumstances. The lack of complete agreement, perhaps due to slight relative shifts perpendicular to the dispersion, fractional-pixel shifts along the dispersion, or differences in exposure level, indicates that the technique is not perfect, and that care will still be needed in the interpretation of weak features.

B. Characteristics of the fixed pattern

Table I contains information on template star spectra which has been accumulated in the course of constructing templates for various projects. The first section of the table gives values for the rms fluctuations (with respect to unity) for typical individual spectra (ind), for the sums of spectra which have (div) or have not (sum) been divided by the template, for the template (tmp), and for an estimate of the random noise in a typical individual spectrum ($\text{rnd} = [\text{ind}^2 - \text{tmp}^2]^{1/2}$, which assumes that the random noise and FPN are uncorrelated). These rms values may be converted to (2σ) equivalent width limits or error bars by using the formula $W_\lambda = 2 \times \text{rms} \times \Delta\lambda \times n^{1/2}$, where $\Delta\lambda$ is the pixel spacing and n is the number of pixels per resolution element. The S/N may be simply estimated as $1. / \text{rms}$. Thus an rms value of .02 typically corresponds to $W_\lambda \sim 4 \text{ m}\text{\AA}$ and to a S/N of 50. The singly-exposed SWP and LWP spectra are from η UMa PHCAL images obtained from the IUE archives. The multiply-exposed SWP and LWP spectra are from images of η UMa optimized near orders 68 ($\lambda 2025$) and 81 ($\lambda 2850$), respectively. The multiply-exposed LWR spectra are from images of η Lup optimized near order 100 ($\lambda 2325$). Though this table is not a

comprehensive description of the noise in IUE spectra, a few general trends may be noted.

First, all the rms values seem to increase with increasing order number (decreasing wavelength). This may just be a consequence of decreasing flux at the shorter wavelengths; it would be necessary to examine the corresponding average DN in the raw images. Second, the multiply-exposed spectra have generally lower rms values than the singly-exposed spectra, as would be hoped from having more photons per image. Third, the noise in the template spectra (i.e. the FPN) seems to be comparable to (usually slightly less than) the estimated random noise for a single spectrum - so that removing only the FPN or the random noise would typically not yield more than a factor of about 1.5 increase in the S/N over what is available from a single image. That the rms values for the sums of spectra not divided by the template are typically a factor of two to three smaller than those for the individual spectra indicates, however, that there is generally some cancellation of the FPN even in the sums of undivided spectra. Finally, the rms values for the sums of spectra divided by the template are substantially smaller than for the sums of undivided spectra, and are consistent with random noise reduced by the square root of the number of spectra summed. For these cases, where the templates were constructed (as shifted sums in pixel space) from the same spectra which were summed (in wavelength space, divided by the shifted template), the FPN has apparently been essentially removed.

The second section of Table I shows the dependence of the rms values for the template and for summed spectra upon the number of spectra (singly-exposed η UMa) used. The values for the templates and for the sums of undivided spectra do not decrease much when the number of spectra is increased from 5 to 15 - the FPN is the dominant contributor to the template, and apparently limits the practically achievable S/N in the undivided sums. The rms values for the sums of spectra divided by the appropriately shifted template, however, again show a decrease consistent with random noise statistics.

The third section of Table I gives rms values for templates constructed from different stars (all are multiply-exposed; see also figures 2 and 3). The rms values are similar where the spectra are all well-exposed; the greater increase in rms with increasing order for some stars is probably a consequence of their later spectral type (thus reduced flux) - η UMa is B3V, δ Crv is B9.5V, χ TrA is A1V, α Oph is A5III.

Figures 4, 5, and 6 display some of the templates that we have constructed for various regions of the SWP camera. On the left are the templates; on the

right are their Fourier power spectra, which were computed after subtracting 1.0 from the templates and then smoothing the ends with a 10-point cosine-bell filter. Figures 4 and 5 show the similarities between templates constructed from multiply-exposed spectra of η UMa, singly-exposed spectra of η UMa, and multiply-exposed spectra of δ Crv for SWP orders 67 and 68. From these figures, as well as from some cross-correlation experiments, there seem to be definite similarities between templates constructed from multiply-exposed images and those constructed from singly-exposed images where the template star was observed at different offsets perpendicular to the dispersion in the large aperture; there are fewer similarities, however, between the templates constructed from the differently-offset singly-exposed images. Figure 6 shows some other SWP templates constructed from multiply-exposed η UMa spectra. There is apparently some variety in the frequencies of noise present in various orders - even in adjacent orders like 67, where lower frequencies dominate, and 68, where most of the noise seems to be of higher frequency.

C. Application of templates to program star spectra

While it is encouraging that we seem to be able to consistently identify the FP, to construct very similar templates from different stars, and to use templates to apparently essentially remove the FPN from the sums of spectra used to construct the template, the real test of the general usefulness of this technique is whether a template constructed from observations of one star can eliminate (or at least greatly reduce) the FPN in spectra of a different star. In Table II, we present results for some of the spectra we have examined. For each star and each order in the table, three numbers are generally given: rms values for a typical individual spectrum, for the sum of spectra not divided by any template, and for the sum of the template-divided spectra. The use of a template typically reduces the rms in the summed spectra by 10% to 30% (though the improvement can range from essentially none to almost a factor of two); from this limited set of data, it is hard to say whether some stars or some orders are consistently improved more or less, or how the improvement varies with the number of spectra available. It does not seem, however, as if the FPN has been quite as effectively removed as in the cases in Table I (where the template and program stars were one and the same), though the improvement might be greater for some stars if more spectra were available. Again, there is apparently some "accidental" cancellation of the FPN in the sums of undivided spectra, but such cancellation is not predictable, and will generally happen only

for the higher frequency components of the FPN.

Aside from reducing the general noise in IUE spectra, the other main advantage of using this technique is the elimination of spurious weak "features" from the data, and the enhancement of genuine weak features. A few examples are shown in Figures 7 through 12. The left hand part of Figure 7 shows a portion of SWP order 68 for 49 Ori - at the bottom is the sum of 6 undivided spectra, in the middle is the sum of the template-divided spectra, and at the top is the template that was used. To the right are the respective Fourier power spectra. Most of the higher frequency noise seen in both the undivided sum and the template has been removed in the divided sum. Figure 8 shows a part of SWP order 67 for α TrA; here it is mostly lower frequency noise and associated spurious features that have been removed (see also Figures 2 and 4). Figure 9 shows the Mg I λ 2852 line in LWP order 81 of δ Crv. In the undivided spectrum, the line is only one of several possible "features" of comparable strength; its reality is more apparent in the template-divided spectrum, even though it, too, has been slightly "weakened". In each of these three figures, common features, presumably due to the FP, may be noted in comparing the undivided spectra with the templates (and see also their power spectra).

Figures 10 and 11 illustrate some of the improvement possible for weak lines in noisy spectra. The former presents the region near the C IV λ 1548, λ 1551 doublet in SWP order 89 of V Pup. In the middle is the sum of 6 undivided spectra, at the top the sum of the divided spectra. The noise has been reduced by "only" 10%, but the weaker λ 1551 line is much better defined. Figure 11 shows a portion of SWP order 90 near the Si II* λ 1533 line in HR 2142. Here the noise has been reduced by less than 10%, yet the weak λ 1533 line is clearly present in the top (divided) spectrum, whereas it would have been hardly detectable in the undivided summed spectrum at the bottom.

Finally, in Figure 12 we show the results of applying this technique to a section of SWP order 74 near the Al III λ 1863 line in the spectra of SN1987a and in the template star η UMa. In both cases, the undivided spectrum is at the bottom, the divided spectrum is in the middle, and the template is at the top. There are noticeable changes in the inferred interstellar Al III absorption lines toward the supernova after division by the template, with a potentially significant effect on the derived properties of the gas producing those lines. Most, if not all, of the FPN has been removed from the η UMa divided sum, yielding a much cleaner high resolution stellar spectrum.

IV. Conclusions and questions

Our experience with using this template technique to improve the S/N in IUE high-dispersion spectra suggests several general conclusions. First, there is a persistent fixed pattern which is reliably identifiable and very similar in the spectra of different objects obtained at widely separated times. This FP introduces noise into the spectra at a level comparable to the random noise present in a well-exposed individual image, so that substantial improvement of the S/N will require removal of both kinds of noise. Second, the use of template spectra can substantially reduce the FP contribution to the noise in IUE spectra. We have typically obtained a S/N \sim 50 for the sum of 5 to 6 well-exposed high-dispersion spectra by this technique (vs. S/N \sim 40 for undivided sums and S/N \sim 20 for individual spectra). Third, while this technique can greatly enhance the reliable identification of weak features in the spectra, care must still be exercised, as there does not seem to be perfect agreement in the FP seen in different spectra. Fourth, while our first applications of this technique used trailed and multiply-exposed spectra specially observed for that purpose, we have subsequently used the technique with comparable success on normal, singly-exposed images from the IUE archive. This suggests that more precise and sensitive results might be obtainable from many of the archival spectra through the application of appropriately constructed templates. The technique will probably produce the most improvement where there is a small number of program star spectra observed within a short period of time or where there are spurious features due to low-frequency components of the FP, in which cases much of the FPN is likely to survive a simple (undivided) co-addition.

In order to assess the general utility of this potentially powerful technique, however, several questions should be investigated. What is the source of the FP? Is the FPN additive or multiplicative in its effect? What, if any, is its dependence on exposure level - or on other factors? How consistent is the FP, and what are the reasons for any changes? Finally, this technique as currently implemented requires a fair amount of user interaction and judgment - how amenable is it to more automated application?

I am particularly grateful to NASA for its support of the projects upon which this investigation has been based, to the IUE and RDAF staff for their assistance in obtaining the archival images, and to D. G. York for his continued support and useful input.

V. References

- Adelman, S. J. and Leckrone, D. S. 1985, NASA IUE Newsletter **28**, 35.
Frisch, P. C., York, D. G., and Fowler, J. R. 1987, Ap. J. **320**, 842.
Frisch, P. C., York, D. G., and Welty, D. E. 1988, in preparation.
Grady, C. A. and Imhoff, C. L. 1985, NASA IUE Newsletter **28**, 86.
Howarth, I. D. and Phillips, A. P. 1986, M.N.R.A.S. **222**, 809.
Welty, D. E., York, D. G., and Hobbs, L. M. 1986, P.A.S.P. **98**, 857.
York, D. G. and Jura, M. 1982, Ap. J. **254**, 88.
York, D. G., Frisch, P. C., and Welty, D. E. 1988, in preparation.
York, D. G., Polidan, R., and Welty, D. E. 1988, in preparation.

Table I. Noise in Template Spectra

		multiple						single						
order	range	n	ind	sum	div	tmp	rnd	range	n	ind	sum	div	tmp	rnd
SWP 67	2058.0-2066.0	213	.035	.020		.023	.026	2060-2069	213	.035			.019	.029
68	2022.0-2029.0	189	.035	.015		.025	.024	2023-2032	244	.038	.017	.008	.023	.030
74	1853.0-1858.0	140	.041	.019		.027	.031	1860-1869	265	.050	.022	.009	.030	.040
76	1805.5-1811.0	162	.041			.028	.030	1805-1814	267	.050	.023	.008	.032	.038
76	1813.0-1821.0	241	.045	.018		.026	.037							
79								1739-1748	280	.060	.027	.010	.037	.047
79								1749-1757	249	.070	.028	.012	.042	.056
86	1604.0-1610.5	222	.085	.030		.052	.067							
89	1544.0-1554.0	350	.096	.032	.019	.064	.072							
90	1523.0-1530.0	240	.125	.047	.022	.105	.068	1523-1531	275	.125	.040	.017	.087	.090
90	1530.0-1538.0	286	.100	.036		.065	.076	1530-1538	285	.115	.039	.014	.081	.082
LWP 81	2849.0-2857.0	162	.048	.023		.035	.033	2849-2862	262	.058	.017	.010	.038	.044
89	2582.0-2590.0	177	.072	.031		.053	.049							
LWR 76	3039.0-3051.0	224	.062	.026		.043	.045							
76	3049.0-3062.0	243	.057	.022		.038	.042							
77	3013.0-3023.0	189	.052			.037	.037							
78	2960.0-2970.0	191	.080			.065	.047							
97	2370.0-2386.0	382	.12	.051		.096	.072							
98	2360.0-2370.0	242	.067	.031		.049	.046							
99	2321.0-2329.0	192	.14	.066		.120	.072							
100	2321.0-2326.5	133	.10	.042		.063	.078							
101	2290.0-2302.0	298	.091			.068	.060							
102	2257.0-2267.0	253	.142			.122	.073							

4C

number of spectra: 15 Eta UMA (SWP multiple, SWP single, LWP single), 11 Eta UMA (LWP multiple), 14 Eta Lup (LWR multiple)

order	range	ind	sum	div	tmp	rnd
			5/10/15	5/10/15	5/10/15	
SWP 67	2060-2069	.035			----/.021/.019	.029
68	2023-2032	.038	.018/----/.017	.012/----/.008	----/----/.023	.030
79	1739-1748	.060	.030/----/.027	.019/.012/.010	.041/----/.037	.047
79	1749-1757	.070	.035/----/.028	.023/----/.012	.048/----/.042	.056
90	1523-1531	.125	.055/.047/.040	.034/.022/.017	.090/.085/.087	.090

order	range	Eta UMA	Del Crv	Gam TrA	Alp Oph
SWP 67	2058.0-2066.0	.023	.023	.025	.021
68	2022.0-2029.0	.025	.027	.027	.026
74	1853.0-1858.0	.027	.024	.030	.032
76	1805.5-1811.0	.028	.027	.036	.038
86	1604.0-1610.5	.052	.063	.085	
90	1523.0-1530.0	.105	.125		

number of multiply-exposed spectra: 15 Eta UMA, 11 Del Crv, 8 Gam TrA, 10 Alp Oph

n: number of points
ind: rms in typical individual spectrum
sum: rms in sum of all spectra
div: rms in sum of all divided spectra
tmp: rms in template
rnd: calculated random noise in typical individual spectrum (rnd**2 = ind**2 - tmp**2)

Table II. Noise in Program Star Spectra

star	ns/nl	SWP 67	SWP 68	SWP 74	SWP 76	SWP 86	SWP 90	LWP 81	LWP 89
Eta UMa	12/11	.035/.020/-----	.035/.015/-----	.041/.019/-----	.041/-----/-----	.085/.030/-----	.125/.047/.022	.048/.023/-----	.072/.031/-----
49 Ori	6/10	.033/.019/.016	.035/.016/.012	.046/.025/.020	.056/.028/.023			.062/.023/.025	.160/-----/-----
232 Pup	1/ 3	.033/.033/.031	.039/.039/.028	.041/.041/.035	.053/.053/.050	.127/.127/.124		.070/.037/.033	----/.058/.057
Del Crv	7/ 9 11/ 0	.032/.020/.015 .032/.020/.016	.035/.021/.019 .034/.018/.016	.040/.024/.020 .036/.019/.018	.043/.026/.023 .040/.021/.023	----/----/.049 .092/.043/.030	.180/----/---- .145/.086/.065	.056/.023/.017	.085/.032/.029
Gam TrA	3/11 8/ 0	.040/.027/.021 .035/.023/.013	.039/.018/.019 .035/.019/.016	.054/----/.032 .040/.024/.016	.055/----/.035 .045/.029/.023	----/----/.074 .110/.065/.054	.220/----/----	.070/.029/.022	.120/.030/.028
Alp CrB	4/ 4	.031/.017/.014	.035/----/.017	.039/.021/.021		----/----/.054	.180/----/----	.058/----/.024	.095/----/.037
Alp Oph	2/ 6 10/ 0	.036/.027/.024 .032/.018/.013	.039/.021/.021 .035/.020/.016	.058/.046/.038 .043/.028/.020	.059/----/.039 .052/.033/.031	----/----/.283 .350/----/----		.068/.031/.028	.105/.054/.045
Gam Oph	1/ 1			.037/.037/.035	.046/.046/.038	----/----/.076	.137/.137/----	.047/.045/.045	.069/.069/.057
2 And	1/ 4	.039/.039/.035	----/----/.038	.051/.051/.049	.052/.052/.050	----/----/.142	.301/.301/----	.070/.040/.035	.125/.059/.052

	ns/nl	SWP 67	SWP 68	SWP 74	SWP 76	SWP 79	SWP 79	LWP 81	LWP 82
SN1987a	4/ 7	.056/.045/.041	.050/.038/.035	.052/.030/.027	.065/.042/.038	.110/.065/.050	.125/.067/.052	.070/----/.029	.080/.037/.027

	nl	LWR 97	LWR 98	LWR 99	LWR 100	LWR 101	LWR 102
Eta Lup	/15	.12 / .051/-----	.067/.031/-----	.14 / .066/-----	.10 / .042/-----	.091/----/-----	.142/----/-----
Rho Oph	/17	.13 / .046/.029	.067/----/.022	.16 / .073/.043	.11 / .045/.034	.15 / .062/.055	.150/.062/.055
Bet Sco	/11		.068/----/.017	.15 / .060/.037	.10 / .035/.033	.095/----/-----	
Zet Oph	/ 3		.073/----/.038				

entries for each column are ind/sum/div; ns and nl are the number of swp and lwp/lwr spectra included

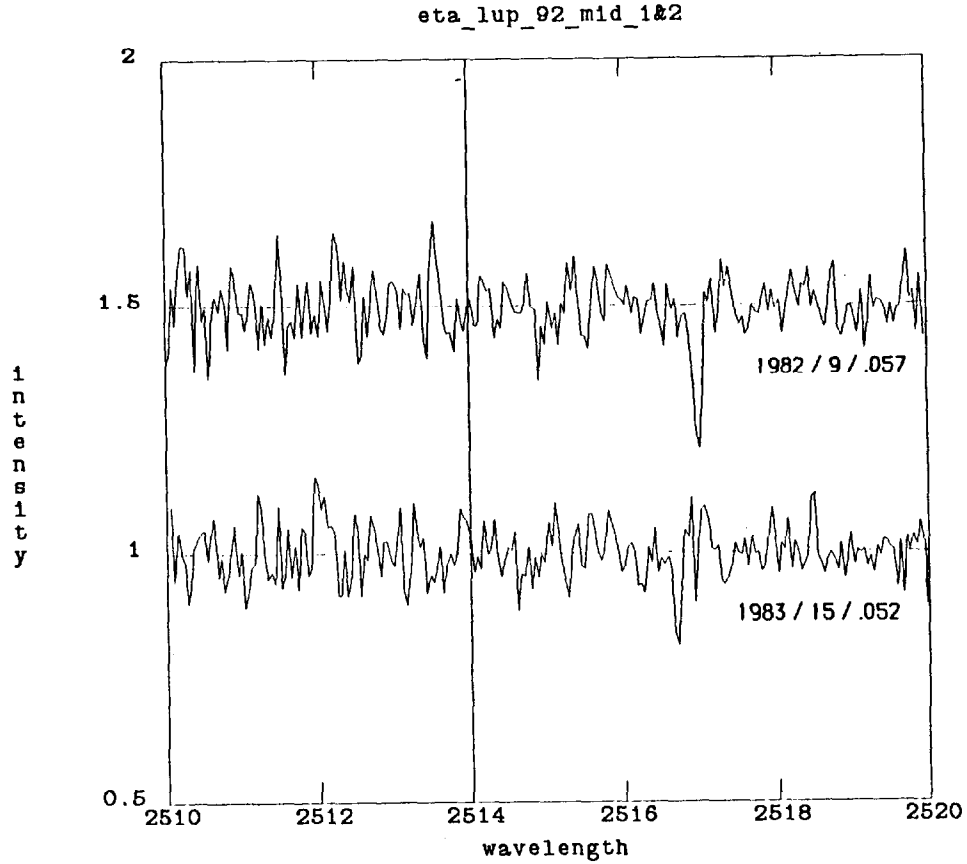


Figure 1. Templates for LWR order 92 constructed from spectra of η Lup obtained during 1982 and 1983. Many common features may be noted. The number of spectra and rms are given for each.

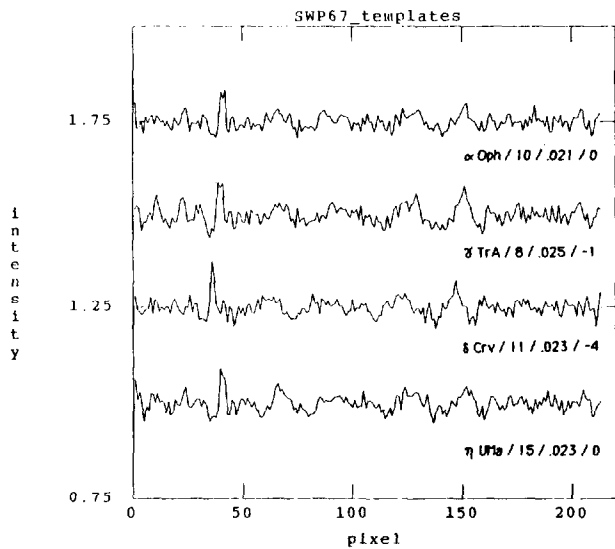


Figure 2. Templates for SWP order 67 constructed from spectra of four stars. Star name, number of spectra, rms, and relative offset are given for each.

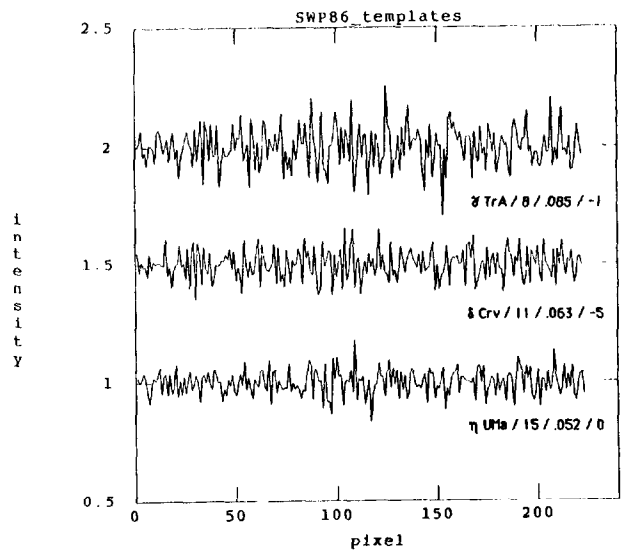


Figure 3. Templates for SWP order 86 constructed from spectra of three stars. The rms is higher and the agreement poorer than for order 67.

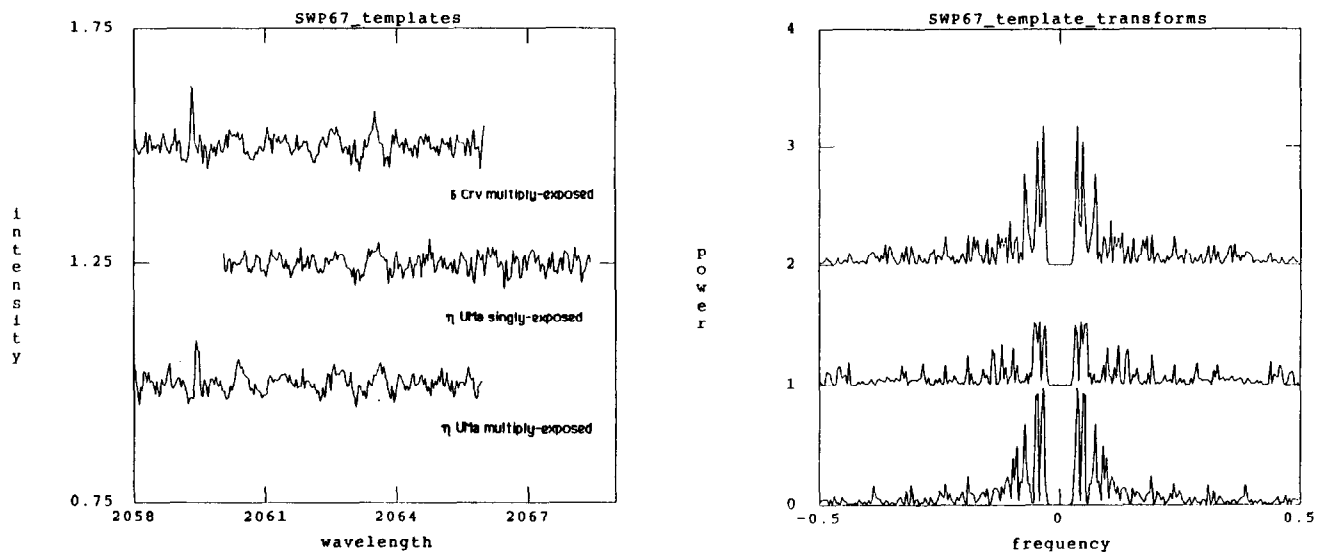


Figure 4. Templates (on the left) and Fourier power spectra (on the right) for SWP order 67. Frequency units are inverse pixels.

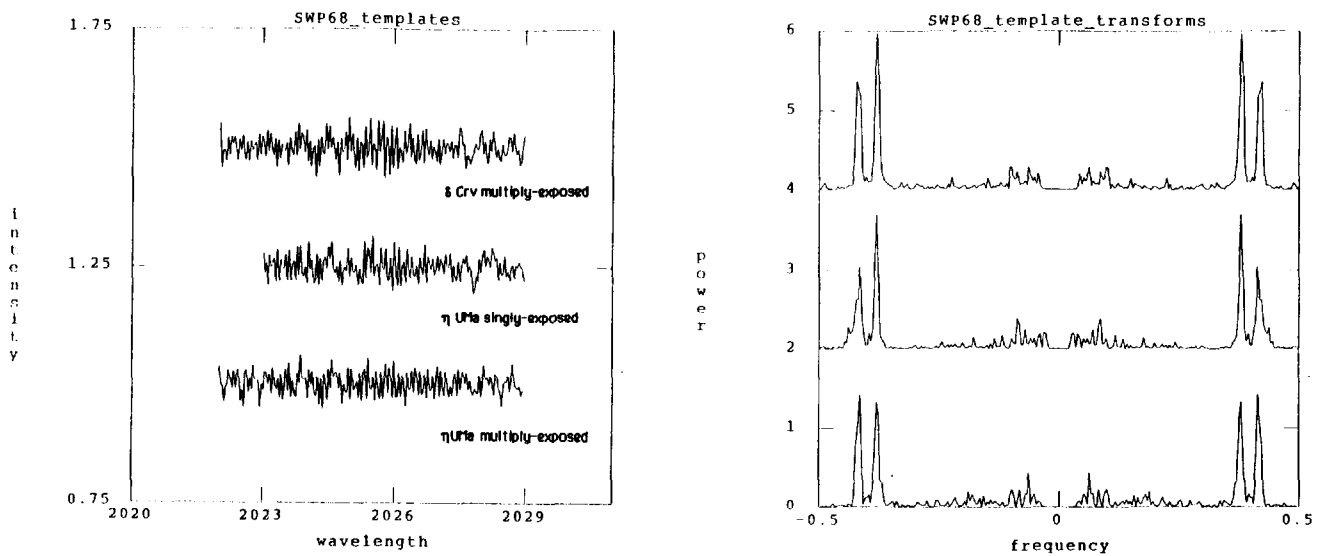


Figure 5. Templates and power spectra for SWP order 68.

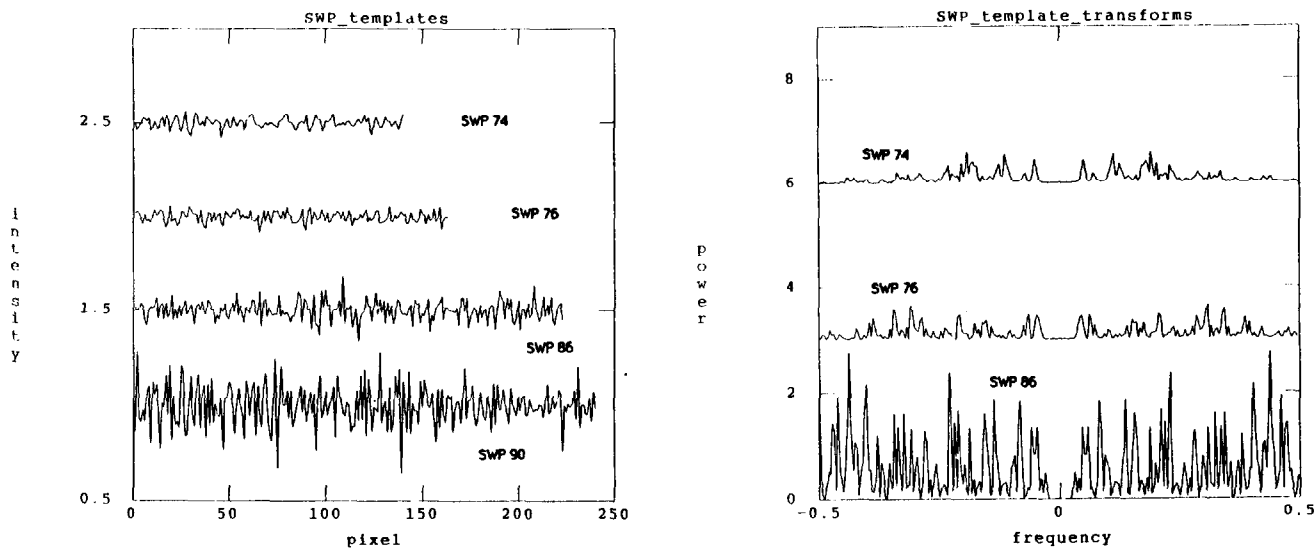


Figure 6. Templates and power spectra for SWP orders 74, 76, 86, and 90 (all multiply-exposed η UMa spectra).

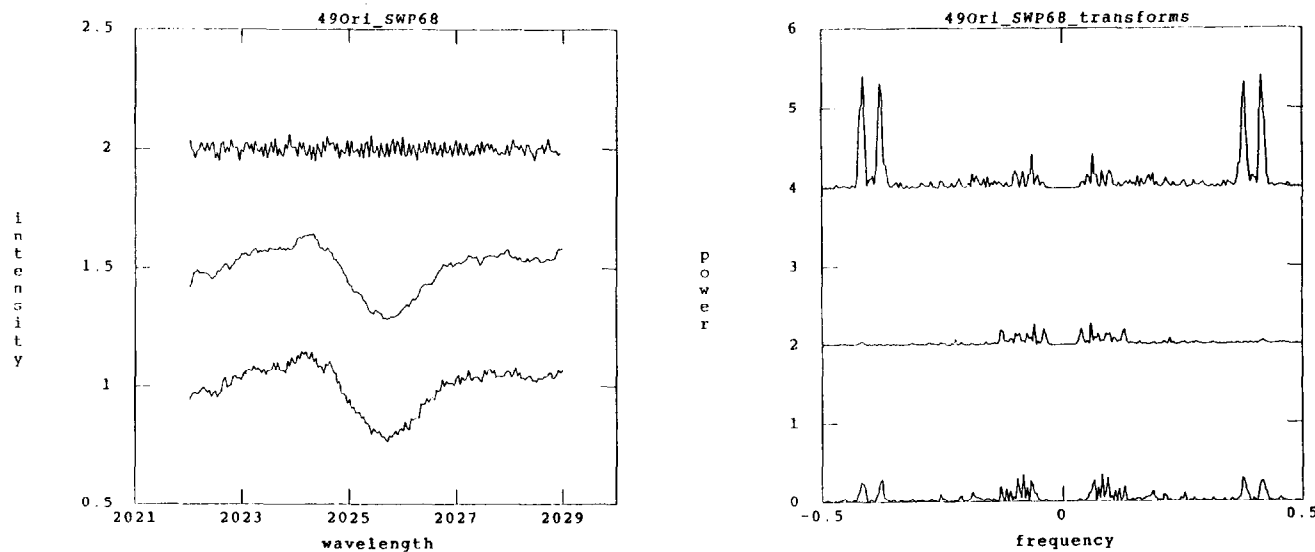


Figure 7. At bottom (left) is sum of 6 undivided spectra of 49 Ori from SWP order 68; in the middle is the divided sum; at the top is the template (η UMa). At the right are the power spectra. Most of the high frequency noise has been removed by the division.

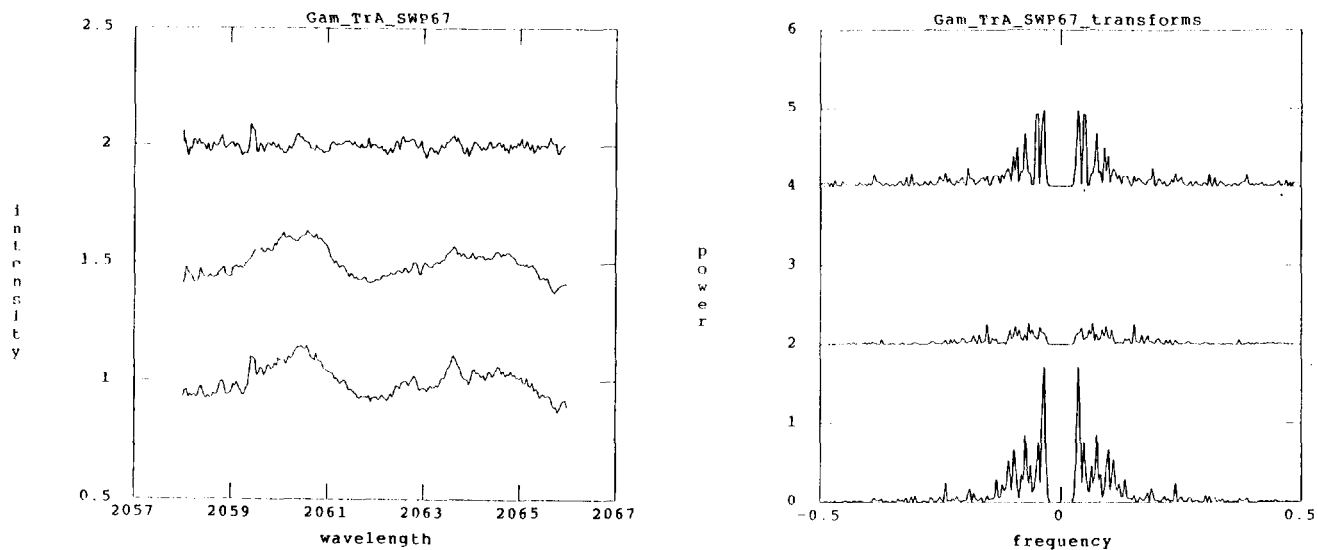


Figure 8. At bottom (left) is sum of 8 undivided spectra of γ TrA from SWP order 67; in the middle is the divided sum; at the top is the template (η UMa). At the right are the power spectra. Much of the low frequency noise has been removed by the division.

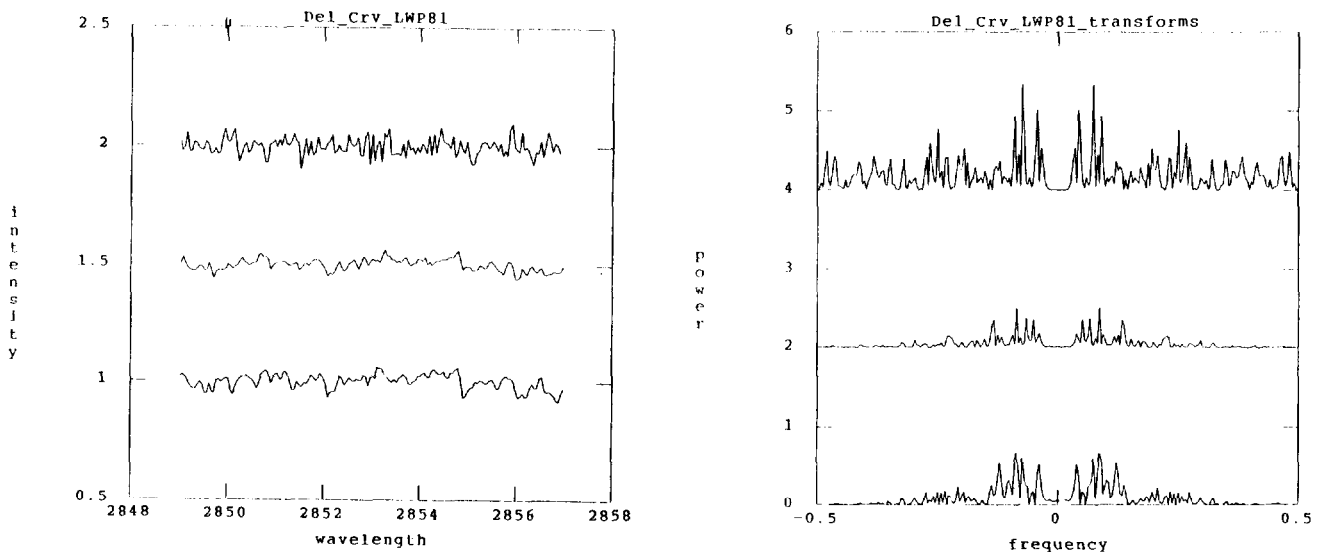


Figure 9. At bottom (left) is sum of 9 undivided spectra of δ Crv from LWP order 81; in the middle is the divided sum; at the top is the template (η UMa). At the right are the power spectra. Much of the low frequency noise has been removed by the division. The Mg I λ 2852 line is enhanced relative to the noise in the divided spectrum.

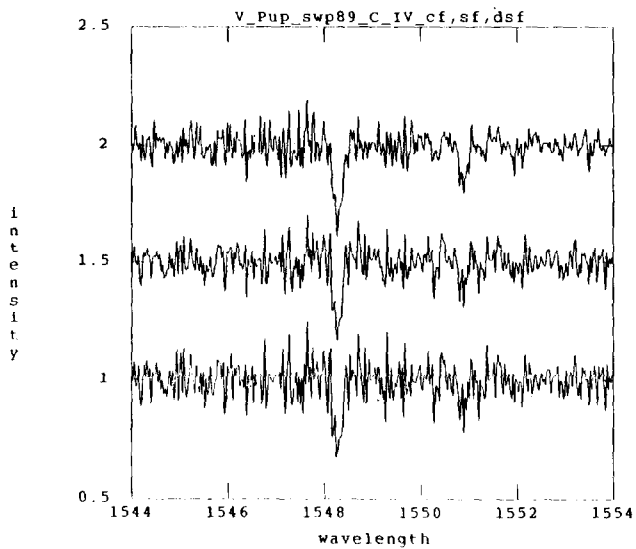


Figure 10. Undivided (middle) and divided (top) spectra of V Pup near the C IV $\lambda 1548, \lambda 1551$ doublet. The weaker $\lambda 1551$ line is much clearer in the divided spectrum.

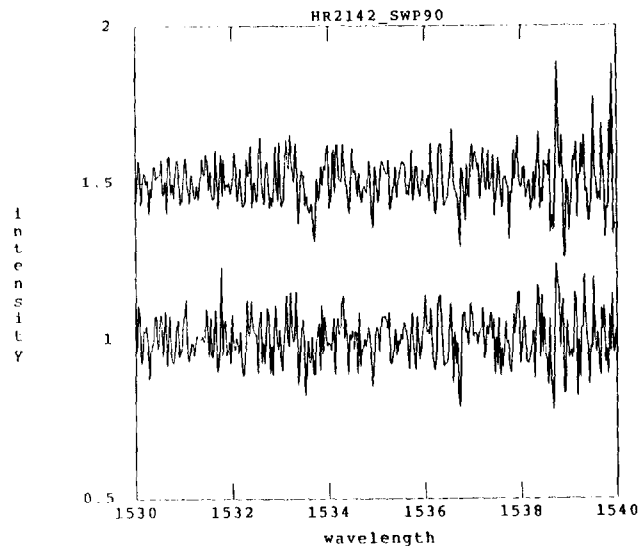


Figure 11. Undivided (bottom) and divided (top) spectra of HR 2142 near the Si II* $\lambda 1533$ line. The line is much clearer in the divided spectrum.

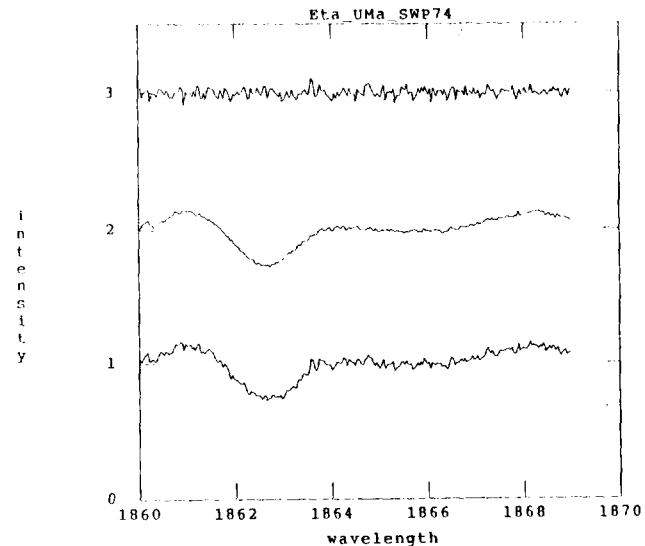
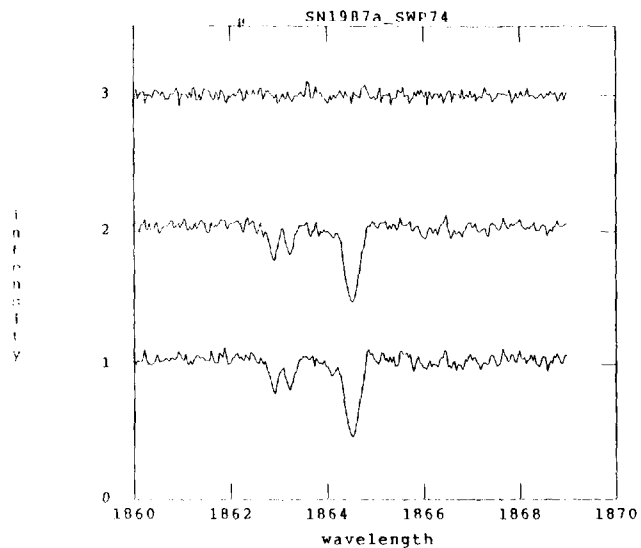


Figure 12. Spectra from SWP order 74 of SN1987a (left) and η UMa (right). At the bottom is the undivided sum; in the middle is the divided sum; at the top is the template (η UMa). Note changes in the interstellar Al III $\lambda 1863$ line profile in the supernova spectrum and the much cleaner stellar spectrum resulting from use of the template.